Article

Effect of Sulfur- and Tar-Contaminated Syngas on Solid Oxide Fuel Cell Anode Materials

Paul Boldrin,*,[†] Marcos Millan-Agorio,[‡] and Nigel P. Brandon[†]

[†]Department of Earth Science and Engineering, and [‡]Department of Chemical Engineering, Imperial College London, London SW7 2AZ, United Kingdom

ABSTRACT: The combination of gasification and solid oxide fuel cells (SOFCs) has the potential to improve efficiency and reduce emissions for fuels, such as coal and biomass. Gasification syngas is a mix of fuel gases containing contaminants, such as sulfur and tar, which have the potential to cause degradation of the materials used in the anode of the SOFC. In this study, nickel−gadolinium-doped ceria (Ni−CGO) composites are exposed to syngas and toluene- and sulfur- (as CS_2) contaminated syngas at temperatures from 600 to 765 °C to investigate the effects of the feed gases and contaminants on their reforming activity and the amount and type of carbon deposited. Under conditions favoring carbon deposition, a two-stage deactivation of the reforming activity is observed, with this being largely the same whether the syngas is pure or contaminated. Toluene-contaminated syngas does not increase the amount of carbon deposited or make it more difficult to remove graphitic carbon compared to uncontaminated syngas below 700 °C, but at 700 °C and above, it does increase the amount of carbon and produce more graphitic carbon. Syngas and toluene appear to compete for active sites, suggesting that the effects of tars and model tars on SOFCs need to be investigated under syngas rather than under hydrogen. Sulfur contamination reduces the amount of carbon deposition above 11 ppm of H_2S.

■ INTRODUCTION

As part of the energy mix in society, it may be necessary to use fuels, such as coal and biomass, which are cheap and widely available, in a way that minimizes their environmental impact. Gasification of these fuels and feeding of the product gas into a solid oxide fuel cell (SOFC) has the potential of high efficiency and low emissions of carbon dioxide and other pollutants compared to their use in conventional power stations.[1−4] The use of gasification products as SOFC fuel has been tested experimentally.[5−7] One of the main issues with the use of gasification feed streams in SOFCs is the detrimental effect that some components of the gas have on the materials used in the anode of the SOFC.[8−10] Gasification feed streams are composed of a mix of hydrogen, carbon monoxide, carbon dioxide, methane, water vapor, and nitrogen as major components, along with contaminants, such as tars and sulfides.[11] Dependent upon the precise composition of the gas, which varies according to the gasification technology employed, carbon deposition can become increasingly thermodynamically favorable below 800 °C. Nickel, the most widely used electrocatalyst in SOFC anodes, is particularly susceptible to deactivation by carbon formation.[12,13]

Carbon deposition can cause damage to the structural integrity of the anode as well as reduce the catalytic activity by poisoning the active sites.[12] Sulfur-containing molecules, such as hydrogen sulfide, reduce the catalytic activity, again by poisoning the active sites.[12,14,15] Similar to carbon deposition, this becomes more of an issue at lower temperatures.[12,15,16]

There are methods for reducing the tar and sulfur contents of gasifier outputs,[17,18] but these require energy and may reduce the heating value of the fuel gas. In addition, carbon monoxide itself can cause carbon deposition in certain conditions.[19,20] Mitigation strategies for carbon deposition at the fuel cell itself include a high concentration of steam[21,22] to promote tar

reforming or avoiding low current density[23] to maintain high oxygen fluxes. These strategies seek to maintain the SOFC anodes in a thermodynamic regime, where carbon deposition should not occur, albeit previous experiments have shown that tars can cause the formation of carbon deposits even outside the envelope of operating conditions, where it would be favored.[24−26]

The effect of aromatic compounds, including tars, on operating SOFCs has recently been comprehensively reviewed.[27] In general, these studies run the SOFC under conditions where carbon deposition is not predicted thermodynamically, for example, at high temperature and under load. Those studies using state-of-the-art nickel−gadolinium-doped ceria (Ni−CGO) anodes show a low impact of tar under these conditions. Estimates of levels of tar that do not affect the SOFC performance range from >10 g m^{-3} [28] to 20 g m^{-3},[29] while a further study showed that naphthalene could affect both the performance of the cell and the reforming reactions in the cell at concentrations around 2000 ppm.[30]

During the operation of a SOFC, there may be occasions where mitigation strategies fail or cannot be used and the SOFC anode is exposed to conditions where carbon deposition is thermodynamically predicted. This work seeks to examine the impact of tar and sulfur on Ni−CGO cermets commonly used in SOFC anodes under these conditions, following previous studies[21−24,26,31] on the effect of tars at higher temperatures (765 °C). A simulated gasification feed containing a model tar (toluene) and a sulfur compound (carbon disulfide) was used. The use of toluene as a tar model has

been proven to represent a worse-case scenario in terms of the tendency to form carbon deposits. Actual gasification tars were found to have a less detrimental effect on SOFC anodes.[24−26] The combined effect of toluene and sulfur on the catalytic activity of the anode materials and the amount and type of carbon deposited is presented in this study.

Our experimental approach studies the effects of syngas and contaminants on the fuel cell materials outside of a cell. The main advantage of this approach is that the amount of carbon produced is much larger than would normally be produced in a SOFC anode, and therefore, the amount and types of carbon deposited can be assessed. A further advantage is that the baseline catalytic activity of the anode materials can be more easily separated from the effects of other cell components (e.g., current collectors) and electrochemical effects. These results should be directly transferable to fuel cells at open circuit voltage and regions of anodes outside the electrochemically active area, although electrochemically active regions may see some differences.

■ EXPERIMENTAL SECTION

Thermodynamic calculations were performed using National Aeronautics and Space Administration (NASA) Chemical Equilibrium with Applications (CEA) code. Commercial NiO−CGO powder (NiGDC-P, lot number 5A073, 60 wt % NiO and 40 wt % $Ce_{0.9}Gd_{0.1}O_{1.95}$, with a surface area of 5.2 m^2/g, purchased from Fuel Cell Materials, Columbus, OH) was calcined at 1300 °C for 1 h. The testing apparatus has been described previously.[21] A total of 0.2 g of the calcined material was placed in a quartz reaction tube and held in place by quartz wool, which was then placed into a furnace. One end of the tube was attached to mass flow controllers, such that the sample could be supplied with the reaction gases via a preheater for introduction of water or organic vapors, while the other end was attached to a mass spectrometer to measure the outlet gas composition. The material was heated at 10 °C min^{-1} under 100 mL min^{-1} dry Ar to 765 °C. Upon reaching this temperature, the gas was switched to 100 mL min^{-1} 10% H_2 in Ar, humidified at 20 °C (hence, containing 2.3% H_2O). Ar was used instead of N_2 to avoid interference with the determination of CO by mass spectroscopy. After 30 min, the temperature was changed to that of the reaction and the gas was switched to a 100 mL min^{-1} flow containing 60% Ar, 15% H_2, and 25% CO, again humidified at 20 °C, giving a steam/carbon (S/C) ratio of 0.092. Optionally, 100 μL h^{-1} toluene (S/C = 0.084) or a toluene−carbon disulfide mixture (S/C = 0.084) was injected using a syringe pump into the preheater, kept between 150 and 200 °C. The reaction was run for 1 h, and the gas composition was measured continuously. At the end of the hour, the gas was switched to 100 mL min^{-1} 10% H_2 in Ar, the syringe pump switched off, and the reactor cooled. Once the temperature dropped below 200 °C, the gas was changed to 100 mL min^{-1} 2% O_2 in Ar and the reactor was heated to 1000 °C at 5 °C min^{-1}, again using mass spectrometry to measure the gas composition.

■ RESULTS AND DISCUSSION

In fuel cell anodes powered by syngas, there are a number of reactions occurring that are important to the functioning of a fuel cell, such as the water−gas shift and reforming reactions. While these reactions are complex, when the outlet gas of the reactor is monitored, it is possible to estimate how the presence of toluene and sulfur affect them. It is well-known that carbon monoxide can cause carbon deposition at lower temperatures, which adversely affects the catalytic and electrocatalytic activities of the anode materials as well as fuel cell performance and lifetime. Figure 1 shows the thermodynamic equilibrium for the conditions used in these experiments. As the
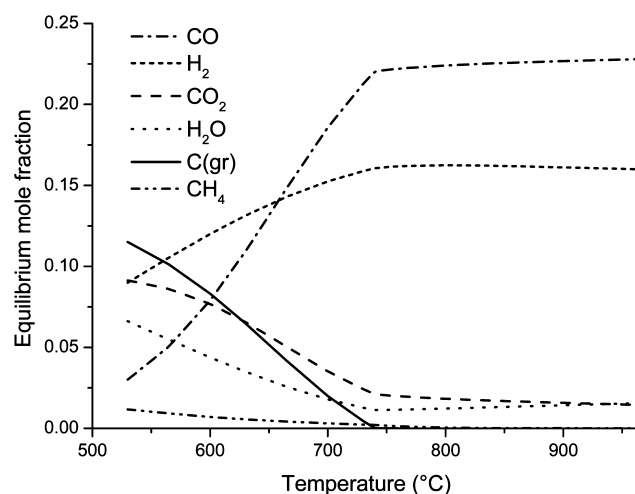
Figure 1. Thermodynamic calculations for 15% H_2, 25% CO, 2% H_2O, and balance Ar showing the expected equilibrium concentrations at a range of temperatures.

temperature decreases, more CO_2, H_2O, CH_4, and solid carbon are produced, while CO and H_2 concentrations decrease.

A sense of how the activity of the catalyst evolved over time was obtained by examining the amount of CO_2 produced by water−gas shift. Figure 2a shows traces of CO_2 production at temperatures ranging from 600 to 765 °C in experiments without toluene. The initial CO_2 production increased with decreasing the temperature, as would be expected from thermodynamics. However, the lower temperatures showed a large drop in activity over the first few minutes, with further decreases up to 30 min. This is indicative of deactivation because of carbon deposition. At 765 °C, there was no decline in activity, indicating that, as suggested by the thermodynamic calculations, carbon deposition does not occur.

Experiments conducted with toluene in the gas feed gave similar results, shown in Figure 2b. As before, the higher CO_2 production was seen at lower temperatures, and there was also a two-stage decrease in the activity of the samples at 600, 650, and 700 °C. There was a slight deactivation seen in the sample exposed to toluene at 765 °C, indicating some carbon deposition, although at this temperature, this is not predicted by thermodynamics, in line with previous observations.[21−23]

In general, for both sets of samples, the deactivation is slower at lower temperatures, indicating that the rate of carbon deposition is determined by the slower kinetics at reduced temperatures rather than the thermodynamic driving force toward carbon deposition. The levels of activity and deactivation were not significantly different with and without toluene at 600 or 700 °C, but there was some difference at 650 °C, where the deactivation was slower in the sample exposed to toluene. In this sample, the decline in activity was similar to that seen at 600 °C, which is an indication that, at this temperature, the presence of toluene is hindering the rate of carbon deposition.

Temperature-programmed oxidation (TPO) of these samples showed the extent of carbon deposition. TPO involves the controlled oxidation of the sample in an atmosphere preventing self-sustaining oxidation, with the amount of carbon deposited able to be measured by monitoring the emission of CO_2 by mass spectrometry. Figure 3 shows the amount of carbon deposited, normalized against the total mass of the unreduced catalyst, at different temperatures with and without toluene.
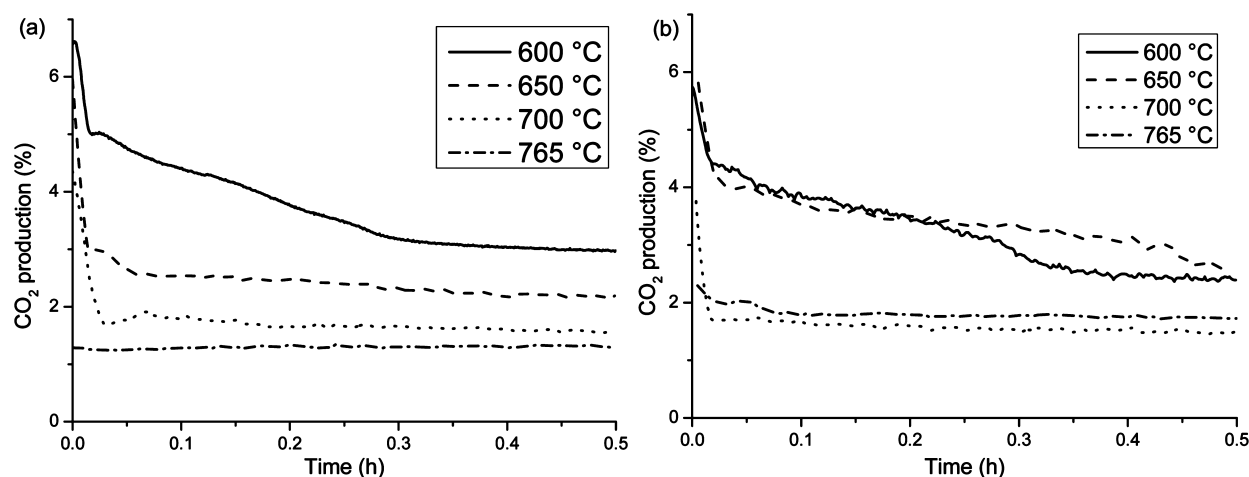
Figure 2. CO_2 production from syngas passed over Ni−CGO at different temperatures (a) without toluene or (b) with toluene.
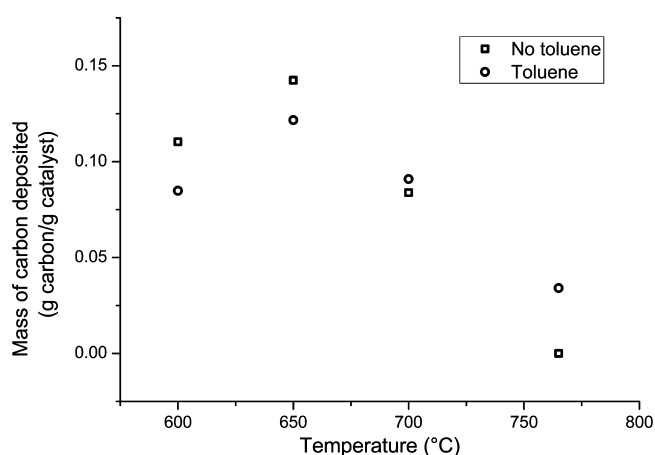

Figure 3. Mass of carbon deposited on Ni−CGO exposed to syngas with or without toluene for 1 h at a range of temperatures.

There was no carbon deposited at 765 °C without toluene, which is in agreement with the observations on the evolution of CO_2 and the thermodynamic calculations shown in Figure 1. Interestingly, a previous study by our group using the same equipment and experimental conditions[24] found a higher level of carbon deposition using toluene and hydrogen (0.07 g of

carbon g^{-1} of unreduced catalyst h^{-1}) than in this study using toluene and syngas (0.034 g of carbon g^{-1} of unreduced catalyst h^{-1}) at 765 °C. This indicates that the presence of carbon monoxide hinders carbon deposition, possibly by blocking sites for toluene adsorption, a similar effect to that shown in an earlier study, where the addition of 10% CO_2 to a mixture of benzene in 15% H_2 (balance N_2) led to a decrease in the amount of carbon deposits.[22]

As expected from thermodynamics, the amount of carbon deposited both with and without toluene increased as the temperature decreased from 765 to 700 and 650 °C. The amount of carbon decreases from 650 to 600 °C, indicating that the rate of carbon deposition becomes slower at the lower temperature. Interestingly, the amount of carbon deposited at 600 and 650 °C under syngas and toluene was lower than that under syngas alone, indicating that toluene retards the rate of deposition of carbon at these lower temperatures and reinforces the view that there is a competition between the adsorption of toluene and CO on the Ni−CGO catalyst.

As well as the overall amounts of carbon deposited, TPO can provide insight on the types of carbon that have been deposited. As suggested elsewhere,[24] the temperature of production of carbon dioxide (i.e., the temperature that the carbon deposits are oxidized) relates to the crystallinity of
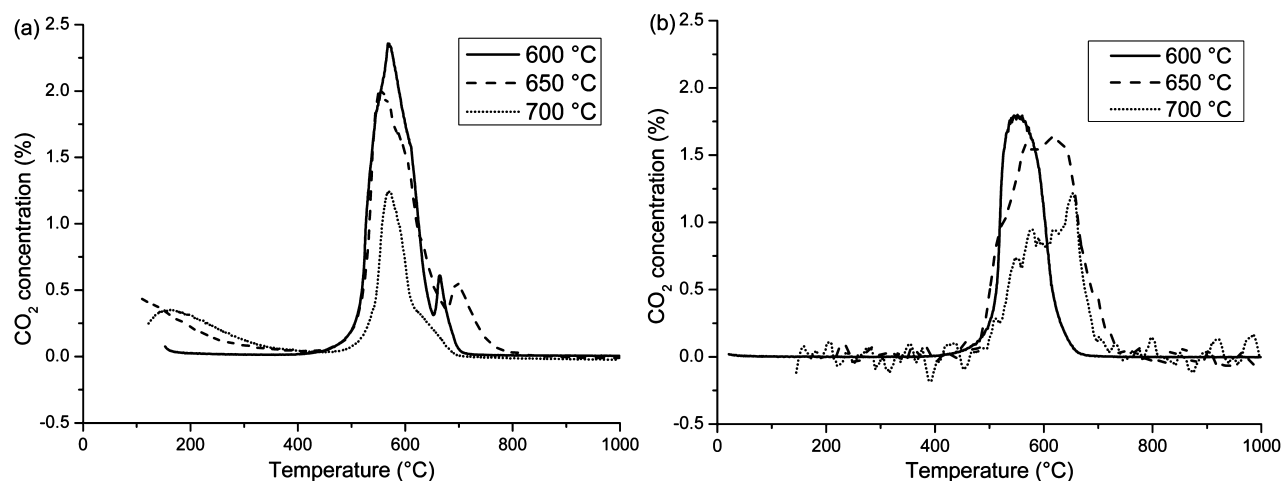

Figure 4. TPO of Ni−CGO exposed to syngas for 1 h at a range of temperatures (a) without toluene or (b) with toluene.

carbon deposited, with carbon dioxide produced at lower temperatures from the oxidation of amorphous carbon, whereas more graphitic carbon requires higher temperatures to oxidize. Figure 4a shows the TPO traces of the samples not exposed to toluene. A high-temperature shoulder, above 650 °C in the TPO experiment, appeared in Ni–CGO samples exposed to the gas mixture at temperatures of 650 °C and below. The presence of the high-temperature shoulder indicates that graphitic carbon can form at lower temperatures, although the proportion of the overall carbon oxidized above 650 °C is very low, meaning that the large majority of carbon formed is amorphous in nature.

In comparison of these to the TPO traces of the samples exposed to syngas and toluene (Figure 4b), it was observed that this high-temperature shoulder was much larger at the higher temperatures, indicating a larger amount of graphitic carbon deposits. Interestingly, this high-temperature peak disappeared at 600 °C, indicating that less graphitic carbon was produced at this lower temperature compared to the samples not exposed to toluene. This suggests that a mix of factors affects the type of carbon deposited under toluene. A further difference was the presence of a very low temperature peak below 300 °C in the samples exposed to syngas without toluene. This is normally attributed to easily oxidized carbon deposited directly on metal particles.[32] This peak was not present in the samples exposed to syngas and toluene.

In summary, these results indicate that, in the presence of syngas in conditions favoring carbon deposition, toluene has a relatively minor effect on the amount of carbon deposited. However, it does affect the type of carbon deposited, with the carbon in general being easier to remove at low reaction temperatures and more graphitic and difficult to remove at higher temperatures. At temperatures where no carbon is deposited in pure syngas, there is still some carbon deposited when toluene is present. Overall, toluene worsens carbon deposition at temperatures above approximately 700 °C.

Following the experiments with syngas and toluene, a model sulfur compound, carbon disulfide, was added by dissolution into toluene. Under the conditions in the preheater, carbon disulfide reacts to form hydrogen sulfide, producing hydrogen sulfide concentrations in the gas stream of 11.3, 28.2, and 56.4 ppm. The amount of carbon deposited at 700 °C was measured, and results are presented in Figure 5. It can be
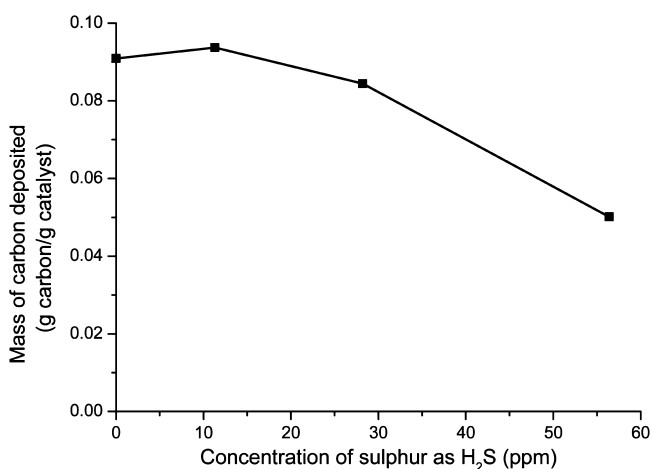
seen that the presence of sulfur at concentrations of 28 ppm and above decreased the amount of carbon deposited, but the amount of carbon deposited was not affected at the lower level of sulfur (11 ppm). Similar results have been seen previously, with the decrease in carbon deposition at higher concentrations being attributed to surface sulfur atoms on nickel blocking the formation of carbon nucleation, while surface sulfur concentrations below a certain level leave large enough bare nickel islands to allow for carbon nucleation.[33−35]

The TPO traces (Figure 6) of the materials after exposure to sulfur- and toluene-contaminated syngas indicate that the
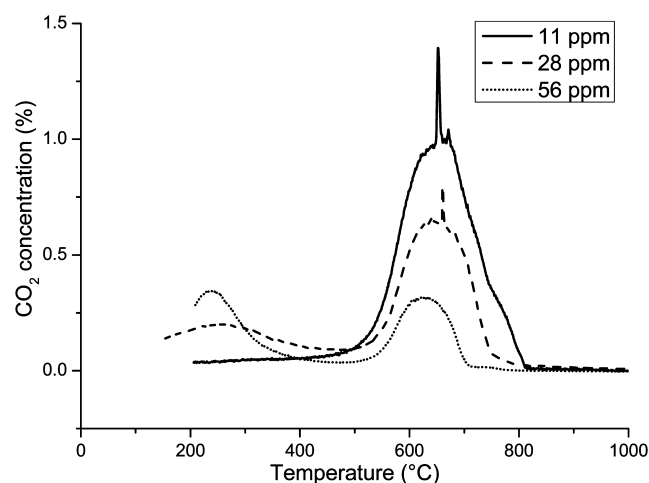
Figure 6. TPO of Ni–CGO exposed to sulfur- and toluene-contaminated syngas at 700 °C.

presence of sulfur reduces the level of graphitic carbon. One further feature was the return of the very low temperature peak, with increasing size as the sulfur content increased. This may result from carbon deposition starting on the metal particles but failing to spread.

■ CONCLUSION

These results indicate that, under conditions where carbon deposition would be expected to occur, the deposition is not worsened by toluene as a model tar. However, in regimes where carbon deposition does not occur under pure syngas, carbon deposition is still observed with toluene. The implications of this in SOFCs when toluene may be present are that the carbon deposition and catalyst degradation caused by operation in regimes that favor carbon deposition are not likely to be worsened by the presence of toluene but that SOFCs operating under regimes that would protect from carbon deposition under syngas will still encounter problems with carbon deposition if there is toluene present. In addition, it appears that toluene and carbon monoxide compete for active sites, suggesting that the effects of tars on operating fuel cells strongly depend upon the overall syngas composition and that results obtained using tar-contaminated hydrogen may not be applicable to tar-contaminated syngas. Finally, it appears that sulfur conveys a protective effect toward carbon deposition at levels above 11 ppm, although sulfur may have effects on the electrochemical reactions, which would require its removal in any case.

Figure 5. Amount of carbon deposited on Ni–CGO exposed to sulfur- and toluene-contaminated syngas at 700 °C.

■ AUTHOR INFORMATION

Corresponding Author

*E-mail: p.boldrin@imperial.ac.uk.

Notes

The authors declare no competing financial interest.

■ REFERENCES

(1) Abuadala, A.; Dincer, I. *Int. J. Hydrogen Energy* **2010**, *35*, 13146−13157.

(2) Di Carlo, A.; Borello, D.; Bocci, E. *Int. J. Hydrogen Energy* **2103**, *38*, 5857−5874.

(3) Kivisaari, T.; Björnbom, P.; Sylwan, C.; Jacquinot, B.; Jansen, D.; de Groot, A. *Chem. Eng. J.* **2004**, *100*, 167−180.

(4) Zhang, X.; Chan, S. H.; Li, G.; Ho, H. K.; Li, J.; Feng, Z. *J. Power Sources* **2010**, *195*, 685−702.

(5) Gasified coal success for Delphi SOFC. *Fuel Cells Bull.* **2003**, *11*, 2.

(6) Singh, R.; Guzman, F.; Khatri, R.; Chuang, S. S. C. *Energy Fuels* **2010**, *24* (2), 1176−1183.

(7) Hofmann, Ph.; Schweiger, A.; Fryda, L.; Panopoulos, K. D.; Hohenwarter, U.; Bentzen, J. D.; Ouweltjes, J. P.; Ahrenfeldt, J.; Henriksen, U.; Kakaras, E. *J. Power Sources* **2007**, *173*, 357−366.

(8) Norheim, A.; Wærnhus, I.; Broström, M.; Hustad, J. E.; Vik, A. *Energy Fuels* **2007**, *21* (2), 1098−1101.

(9) Kee, R. J.; Zhu, H.; Sukeshini, A. M.; Jackson, G. S. *Combust. Sci. Technol.* **2008**, *180*, 1207−1244.

(10) Alzate-Restrepo, V.; Hill, J. M. *J. Power Sources* **2010**, *195*, 1344−1351.

(11) Cayan, F. N.; Zhi, M.; Pakalapati, S. R.; Celik, I.; Wu, N.; Gemmen, R. *J. Power Sources* **2008**, *185*, 595−602.

(12) Offer, G. J.; Mermelstein, J.; Brightman, E.; Brandon, N. P. *J. Am. Ceram. Soc.* **2009**, *92*, 763−780.

(13) Wang, W.; Su, C.; Wu, Y.; Ran, R.; Shao, Z. *Chem. Rev.* **2013**, *113*, 8104−8151.

(14) Schubert, S. K.; Kusnezoff, M.; Michaelis, A.; Bredikhin, S. I. *J. Power Sources* **2012**, *217*, 364−372.

(15) Laycock, C. J.; Staniforth, J. Z.; Ormerod, R. M. *Dalton Trans.* **2011**, *40*, 5494−5504.

(16) Birss, V.; Deleebeeck, L.; Paulson, S.; Smith, T. *ECS Trans.* **2011**, *35*, 1445−1454.

(17) Howard, C. J.; Dagle, R. A.; Lebarbier, V. M.; Rainbolt, J. E.; Li, L.; King, D. L. *Ind. Eng. Chem. Res.* **2013**, *52*, 8125−8138.

(18) Bhandari, P. N.; Kumar, A.; Huhnke, R. L. *Energy Fuels* **2014**, *28* (3), 1918−1925.

(19) Sumi, H.; Lee, Y.-H.; Muroyama, H.; Matsui, T.; Kamijo, M.; Mimuro, S.; Yamanaka, M.; Nakajima, Y.; Eguchi, K. *J. Power Sources* **2011**, *196*, 4451−4457.

(20) Alzate-Restrepo, V.; Hill, J. M. *J. Power Sources* **2010**, *195*, 1344−1351.

(21) Mermelstein, J.; Brandon, N.; Millan, M. *Energy Fuels* **2009**, *23*, 5042−5048.

(22) Mermelstein, J.; Millan, M.; Brandon, N. P. *J. Power Sources* **2011**, *196*, 5027−5034.

(23) Mermelstein, J.; Millan, M.; Brandon, N. *J. Power Sources* **2010**, *195*, 1657−1666.

(24) Lorente, E.; Millan, M.; Brandon, N. P. *Int. J. Hydrogen Energy* **2012**, *37*, 7271−7278.

(25) Liu, M.; Millan, M. G.; Aravind, P. V.; Brandon, N. *J. Electrochem. Soc.* **2011**, *158*, B1310−B1318.

(26) Lorente, E.; Berrueco, C.; Millan, M.; Brandon, N. P. *J. Power Sources* **2013**, *242*, 824−831.

(27) Liu, M.; Aravind, P. V. *Appl. Therm. Eng.* **2014**, *70* (1), 687−693.

(28) Hofmann, Ph.; Panopoulos, K. D.; Aravind, P. V.; Siedlecki, M.; Schweiger, A.; Karl, J.; Ouweltjes, J. P.; Kakaras, E. *Int. J. Hydrogen Energy* **2009**, *34*, 9203−9212.

(29) Ming, L.; van der Kleij, A.; Verkooijen, A. H. M.; Aravind, P. V. *Appl. Energy* **2013**, *108*, 149−157.

(30) Hauth, M.; Lerch, W.; König, K.; Karl, J. *J. Power Sources* **2011**, *196*, 7144−7151.

(31) Mermelstein, J.; Millan, M.; Brandon, N. P. *Chem. Eng. Sci.* **2009**, *64*, 492−500.

(32) Swaan, H. M.; Kroll, V. C. H.; Martin, G. A.; Mirodatos, C. *Catal. Today* **1994**, *21*, 571−578.

(33) Rostrup-Nielsen, J. R. *J. Catal.* **1984**, *85*, 31−43.

(34) Tan, C. D.; Baker, R. T. K. *Catal. Today* **2000**, *63*, 3−20.

(35) Grgicak, C. M.; Green, R. G.; Giorgi, J. B. *J. Power Sources* **2008**, *179*, 317−328.